Journal of Magnetism and Magnetic Materials 444 (2017) 467–471

Contents lists available at ScienceDirect

Journal of Magnetism and Magnetic Materials

journal homepage: www.elsevier.com/locate/jmmm

Research articles

Magnetic particles guided by ellipsoidal AC magnetic fields in a shallow viscous fluid: Controlling trajectories and chain lengths

Guillermo A. Jorge [a,b,*], María Llera [a], Victoria Bekeris [c,d]

[a] Instituto de Ciencias, Universidad Nacional de General Sarmiento, Buenos Aires, Argentina
[b] CONICET – Consejo Nacional de Investigaciones Científicas y Técnicas, Argentina
[c] Universidad de Buenos Aires, Facultad de Ciencias Exactas y Naturales, Departamento de Física, Buenos Aires, Argentina
[d] CONICET-Universidad de Buenos Aires, Instituto de Física de Buenos Aires (IFIBA), Buenos Aires, Argentina

ARTICLE INFO

Article history:
Received 27 June 2017
Received in revised form 17 August 2017
Accepted 19 August 2017
Available online 23 August 2017

ABSTRACT

We study the propulsion of superparamagnetic particles dispersed in a viscous fluid upon the application of an elliptically polarized rotating magnetic field. Reducing the fluid surface tension the particles sediment due to density mismatch and rotate close to the low recipient confining plate. We study the net translational motion arising from the hydrodynamic coupling with the plate and find that, above a cross over magnetic field, magnetically assembled doublets move faster than single particles. In turn, particles are driven in complex highly controlled trajectories by rotating the plane containing the magnetic field vector. The effect of the field rotation on long self assembled chains is discussed and the alternating breakup and reformation of the particle chains is described.

1. Introduction

Dynamical assemblies of superparamagnetic micrometric particles are attracting increasing attention. The mechanisms that govern their dynamics have been extensively examined in the past [1–10]. Particularly, time-dependent magnetic fields have been used to assemble magnetic non active material in a variety of structures [11] and to propel microscopic matter in a fluid medium in motile structures [12]. Arrays might yield highly desired additional degree of control over their properties [13] and satisfy the rising demand for the design of artificial externally controlled structures with direct applications in biomedicine [14–16], in microfluids stirring [17], and in targeted cargo delivery [18,10,19].

Different strategies have been followed. A noticeable example is the self-assembly of complex magnetic microstructures suspended at a water-air interface and subjected to a vertical alternating magnetic field [20,21]. These structures denominated "snakes" arise from the coupling between surface deformations of the fluid and the collective response of particles to an external alternating magnetic field. These deformations bring particles close enough that the head-to-tail dipole-dipole attraction overcomes the repulsion caused by the external field. As a result, chains of particles are formed with resulting magnetic moments pointing along the chains. The chains produce wavelike local motion facilitating the self-assembly process and the component of the magnetic field parallel to the surface of the water further promotes the chain formation and propulsion [21].

At first sight, for particles immersed in a viscous fluid with low Reynolds number, any approach based in the application of AC drives is expected to fail to produce net propulsion because the Navier-Stokes equations become time reversible [22,23]. However, to overcome the challenge of low Reynolds number time reversibility, the interaction between the fluid and a confining plate has been proposed to propel a rotating particle [24].

We address then an arrangement of similar particles as in Ref. [21] but in a fluid where they do not float on the liquid air interface, but sediment due to reduced surface tension and density mismatch in an aqueous dispersion. The particles close to the lower planar surface of the container interact through the fluid with the wall. By applying suitable rotating magnetic fields with controlled time dependent orientation and strength, we find a way to manipulate and propel self-organized microscopic particles forming structures similar to worms assembled or disassembled at will, rotated or transported in any direction of the plane via magnetic control, performing trajectories that can be easily maneuvered. We also focus on the propulsion of single particles and of self assembled particle doublets (dimmers) in the low Reynolds number regime and we examine the response of particle chains. The paper is organized as follows: In Section 2 we describe the experimental set up, and in Section 3 we present first the equations that describe our system

* Corresponding author at: Instituto de Ciencias, Universidad Nacional de General Sarmiento, Buenos Aires, Argentina.
E-mail address: gjorge@ungs.edu.ar (G.A. Jorge).

http://dx.doi.org/10.1016/j.jmmm.2017.08.057
0304-8853/

and following we present the observations and discussion. Conclusions are drawn in Section 4.

2. Experimental

We used as the particle containers, a polystyrene 24-well cell culture plate (Thermo Fisher Scientific®, optically clear, flat bottom), cut in individual wells. The container (15.6 mm in diameter) was filled with a couple of drops (∼ 10 ml) of a diluted deionized aqueous suspension containing magnetic monodisperse 80 μm spherical nickel spheres [20]. Experiments made in homemade containers consisting of a plastic ring, 5 mm inner diameter and 5 mm tall, vertically glued to a microscope glass slide acting as the container's bottom, showed no significant differences. The particles, 80 μm in diameter are still small enough to be suspended over the water surface by surface tension. To examine the dynamics of magnetic particles close to the liquid-glass interface, sedimentation was induced by slightly reducing water surface tension, adding a few μl of isopropyl alcohol. After this procedure, the particles sediment and float at a small distance h above the horizontal plate due to balance between gravity and hydrodynamic forces.

The saturated magnetic moment per particle is 2×10^{-7}A m^2 at a saturation field of about 0.4 T. The magnetic moment per particle in the driving fields used in the experiments ∼10 mT is one order of magnitude smaller [20]. The motion in the container of the individual particles, self-assembled dimmers and chains is monitored with a zenithal digital camera (Nikon® D3100, 24 frames per second), adapted to a stereoscopic microscope (Motic® SMZ 168 TL). We used a commercial LED lamp with variable intensity as a bottom illumination source. The optical setup, located above the coils along the z axis, was provided with a variable zoom (5—200X) and focused close to the solid-liquid bottom interface to record the position of particles as a function of time. For the image analysis, the software ImajeJ [25], CUDA Video Spot Tracker [26] and Tracker Video Analysis Tool [27] were used.

The container was placed in a horizontal glass stage, surrounded by three orthogonal pairs of Helmholtz coils, as shown schematically in Fig. 1. The pair of coils with vertical axis generates a vertical magnetic field, B_z, while the other two pairs with the axes parallel to the x and to the y direction, generate magnetic fields in the x or y direction. The three pairs of coils are 200, 140 and 120 mm in diameter, generating up to 10 mT (with ∼3 mT/A). To apply magnetic fields in the plane perpendicular to the glass slide, either in the $x-z$ or $y-z$ plane, the corresponding coils were powered by a standard two-channel audio amplifier, with each pair of coils connected either directly to a channel or through a capacitor in series in order to form a resonant tandem and lower the circuit impedance. The current in each coil was sensed with an oscilloscope measuring the voltage drop on a 1 Ω resistor in series with the winding. The amplifier is driven by a two-channel Rigol® DG4062 function/arbitrary waveform generator, generating two independent signals with arbitrary frequency, amplitude and phase difference.

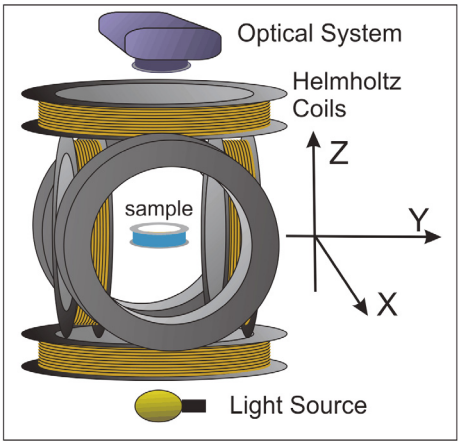

Fig. 1. Schematic view of the experimental setup, showing the three orthogonal pairs of Helmholtz coils, the digital video-microscopy camera and the particle container. See text for details.

After amplification, the magnetic field B_{iz} in the plane i,z with $i = x$ or $i = y$ generated by the setup, is

$$B_{iz} = B_{0i}\sin(2\pi f_i t)\hat{i} + B_{0z}\sin(2\pi f_z t + \theta_{iz})\hat{z}, \quad (1)$$

where B_{0i} and B_{0z} are the AC amplitudes of fields applied in the x (or y) and z direction, f_i and f_z the corresponding frequencies, θ_{iz} is the relative phase between the x (y) and the z field components, which was fixed to $\theta_{iz} = \frac{\pi}{2}$, where $\hat{i}$ and $\hat{z}$ are the versors in the x (or y) and z directions. The ellipticity of the applied field, is $\beta = (B_{0i}^2 - B_{0z}^2)/(B_{0i}^2 + B_{0z}^2)$, with $\beta \in [-1, 1]$. In this paper we limit our discussion to $f_x = f_y = f_z = 50$ Hz, and we therefore define the field angular velocity as $\Omega_B = 2\pi 50$ Hz.

3. Results and discussion

3.1. Rotating and translating spherical particle in a viscous fluid

The equation for the angular motion of a spherical magnetic microparticle in a liquid in the presence of an external rotating magnetic field can be written for negligible Brownian forces, in the following form [28]

$$I\ddot{\varphi} = -\gamma\dot{\varphi} + \mathbf{m}\cdot\mathbf{B}\ \sin(\Omega_B t - \varphi)$$

where I is the moment of inertia of the micro particle of magnetic moment $\mathbf{m}$, φ is the angle of rotation and $\mathbf{B}$ is the applied sinusoidal magnetic field of frequency Ω_B, $\gamma = 8\pi\eta a^3$ is the coefficient of viscous angular drag for a spherical particle of radius a in a fluid with viscosity η.

The microparticle rotation is controlled by the interplay between magnetic and viscous torques and exhibits two distinct modes of motion: synchronous and asynchronous rotation. Synchronous rotation occurs for low angular frequency of the rotating field, Ω_B, because the magnetic and viscous torques are in equilibrium. It has been shown [28] that the critical frequency of the transition from the synchronous to the asynchronous rotational mode, Ω_{crit}, is given by the following expression $\Omega_{crit} = mB/\gamma$. For $\Omega_B \gg \Omega_{crit}$, the average angular frequency of the particles is

$$\Omega = \Omega_B\left[1 - \sqrt{1 - (\Omega_{crit}/\Omega_B)^2}\right] \quad (2)$$

For a sphere of radius 40 μm, with magnetic moment per unit mass 0.614 A m^2 kg^{-1} and typical magnetic field strength $B = 2$ mT, with $\gamma = 2.9\times^{-16}$ N ms for water at room temperature, we get $\Omega_{crit} = 2\pi$ 33 Hz. The applied field rotates at $\Omega_B = 2\pi$ 50 Hz, therefore the particles immersed in an infinite fluid rotate, approximately, with an average angular velocity $\Omega \sim 2\pi$ 12 Hz, with no induced translation [28], and the Reynolds number is $Re = \frac{a^2\Omega}{\nu}$, where ν is the kinematic water viscosity [29], resulting a low Reynolds number, $Re = 0.12$.

However, as the particles are actually located near the bottom, the solid wall induces a coupling between rotational and translational motion. As a result, a net force appears due to an uneven drag force on the top and the bottom surfaces of the particle. In fact, the hydrodynamic interaction between a rotating (or translating) particle of diameter $2a$ and an infinite rigid wall at a distance h

from its surface was studied extensively [24,29] with several approximate expressions for the limiting cases $a/h \gg 1$ or $a/h \ll 1$, which depend on a, h and Ω. As the $x-y$ plane is horizontal, if the particle's angular velocity is $\Omega = \Omega\hat{y}$ ($\Omega > 0$), the presence of the wall is known to yield a net force towards $+\hat{x}$. Changing the polarization of the field by π (*i.e.*, setting $\Omega < 0$) reverses the direction of the net force (towards $-\hat{x}$). There is also a net torque in the same direction of the viscous torque ($-\hat{y}$), changing in this way the angular velocity of the particles. A translating particle in the x direction experiences as well a net opposite force and torque. If the particle's angular velocity lies now in the x direction, the particle displacement results in the $-$y direction. Therefore, particles can be driven to perform controlled complex trajectories by applying magnetic fields with consecutive controlled orientations. In the next subsection we describe our experimental results for single particles, doublets and particle chains.

3.2. Results for single particles, doublets and particle chains

We first address the behavior of single particles in an elliptical magnetic field $B_{iz} = B_{0i}\sin(2\pi 50\,t)\hat{i} + B_{0z}\sin(2\pi 50\,t + \frac{\pi}{2})\hat{z}$ with $B_{0i} = 1$ mT, $B_{0z} = 0.4$ mT ($i = x$ or y).

Panel a) in Fig. 2 shows one of the salient results of this paper, a single particle trajectory after successive $\pm\frac{\pi}{2}$ rotations of the magnetic field plane. For fixed field intensity and frequency, the length of each rectilinear section of the particle trajectory depends on the time interval between successive field rotations, and in the figure linear sections lie in the mm range. With our present set up we can control these trajectories down to ~300 μm, and could be reduced further for lower particle velocities and lower time interval between successive field rotations, providing a strategy for guiding particles, favoring direct applications as targeted drug and cargo delivery or stirring in microfluidic devices.

Occasionally, two particles get close enough so that the dipole–dipole attraction between them forms a steady doublet, and both particles move together in the fluid. Fig. 2 b) shows in full (open) symbols the velocity of single particles (doublets) as a function of B_{0z} for $B_{0x} = 1$ mT. For both single particles and doublets, the velocity increases with B_{0z}, and saturates at $B_{0z} > 0.8$ mT to approximately $v_S \approx 3.0$ mm s^{-1} for single particles and at $B_{0z} > 1.2$ mT to $v_S \approx 6.6$ mm s^{-1} for paired particles. Therefore, the velocity of doublets saturates at about twice the saturation velocity of a single particle, but at low fields there is a crossover and doublets are slower than single particles. Probably, at high B_{0z} the doublets have large enough magnetic moments and one particle can rotate over the other increasing their linear propulsion until it becomes limited by viscous drag. However, a full description of these mechanisms is still lacking. We note that these paired particles differ from the doublets studied by P. Tierno and coauthors [30,31], formed by two micron-size spherical paramagnetic particles with two different radii, coated with streptavidin. In their work, the doublets were dispersed in water and driven by an external precessing magnetic field. In panel c) of Fig. 2 we plot the position as a function of time of two single particles as they merge to form a doublet, increasing their velocity immediately after pair formation. The inset in Fig. 2 c) shows the velocity distribution of single particles in stationary state for $B_{0z} = 0.4$ mT, where the mean velocity is $\overline{V} = 2.6$ mm s^{-1} with a dispersion $\sigma = 0.5$ mm s^{-1}. The spherical particle velocity for fixed Ω_B depends on its diameter $2a$ and on the distance of the particle surface to the wall h [24,29,32]. Therefore the velocity distribution may be related to size, shape and distance to the wall distribution, leading to possible particle merging, as shown in panel c) of in Fig. 2.

We focus now on particle aggregates. It is well known that the interaction between a pair of magnetic particles, k, l at a distance

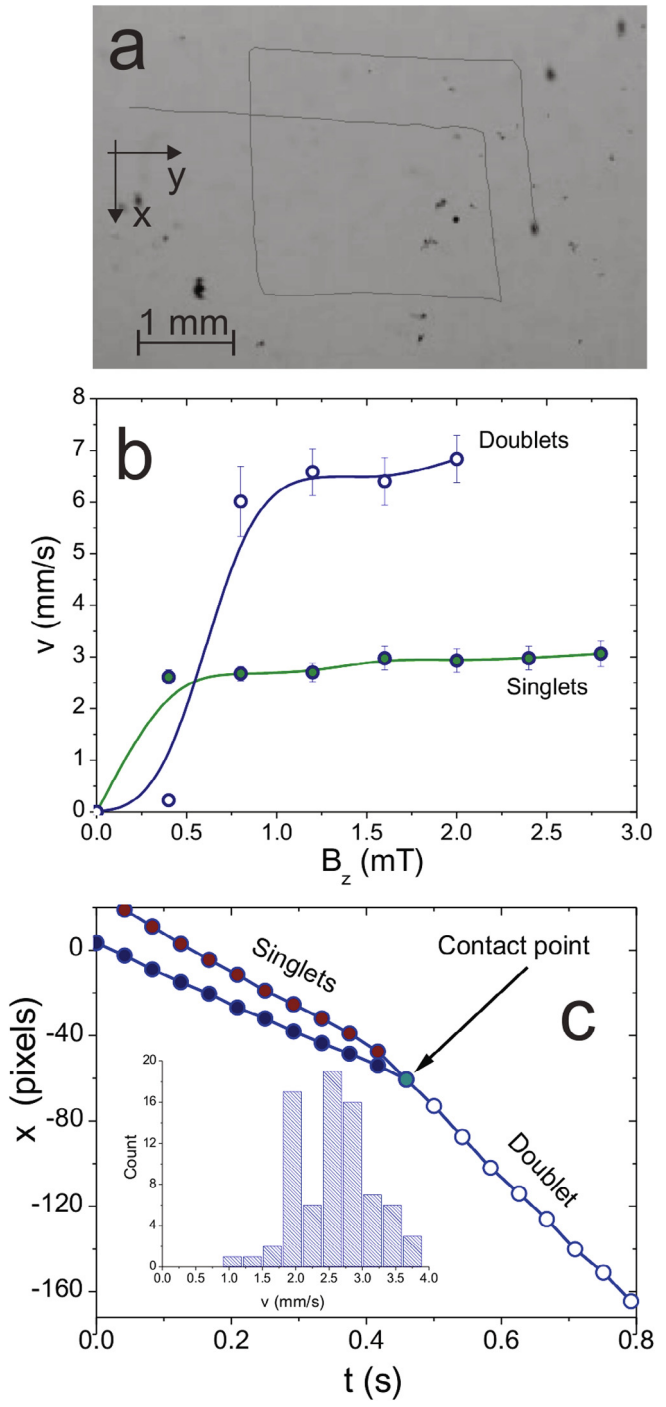

Fig. 2. a) Single particle trajectory after successive $\pm\frac{\pi}{2}$ rotations of the magnetic field plane. b) Steady state velocity, v, as a function of B_{0z} for single particles (full) and doublets (open symbols). c) Position as a function of time for two single particles (full symbols) as they merge to form a doublet (open symbols). See text. Inset: Steady state velocity distribution of single particles for $B_{0z} = 0.4$ mT.

$r_{k,l}$ is maximally attractive (repulsive) for particles with magnetic moments parallel (normal) to $r_{k,l}$. Martinez Pedrero et al. [33] have shown that the average of the dipolar potential energy between two colloids in a rotating magnetic field in the x, z plane is attractive, leading to chain formation along the x direction while single particles in the chain may keep rotating at high enough magnetic fields. In contrast, the effective potential results repulsive in the orthogonal y direction, tending to separate chains. As a result, the application of an elliptical AC field forms elongated agglomer-

ations or chains of paramagnetic particles that show rich dynamical behavior.

We now address the dynamics of self assembled particle chains in an elliptical magnetic field $B_{yz} = B_{0y}\sin(2\pi 50t)\hat{i} + B_{0z}\sin(2\pi 50t + \frac{\pi}{2})\hat{z}$ with $B_{0y} = 1$ mT and $B_{0z} = 0.4$ mT. Fig. 3a) shows a snapshot of the assembled stationary chains. At low fields, long chains are not able to translate, even though single particles or doublets are easily propelled. The mechanism is still an open question, but it is probably related to inhibited rotation of particles in the chain due to long range magnetic interactions. Once the stationary chain formation is achieved, the y field component, $B_y = B_{0y}\sin(2\pi 50t)$, is turned off and the x field component, $B_x = B_{0x}\sin(2\pi 50t)$ with $B_{0x} = B_{0y}$ is applied. This results in the abrupt $\frac{\pi}{2}$ rotation of the plane containing the total applied magnetic field vector, from the $y-z$ to the $x-z$ plane. As shown in Fig. 3 b) the long chains do not rotate to align the particles with the field plane. Instead, the chains break into short fragments that follow the field orientation. Panel b) is a snapshot of the fragmented chains immediately aligned in the new field direction; the inset shows the chain length histogram for this snapshot, with an average length of $(235 \pm 15)\mu$m. Fig. 3 c) is a superposition of both a) and b) snapshots (initial chains in light grey and fragments in dark grey lines) clearly showing the rotation in $\frac{\pi}{2}$ of chain segments around their center of mass and interestingly, keeping their centre of mass in its original chain position.

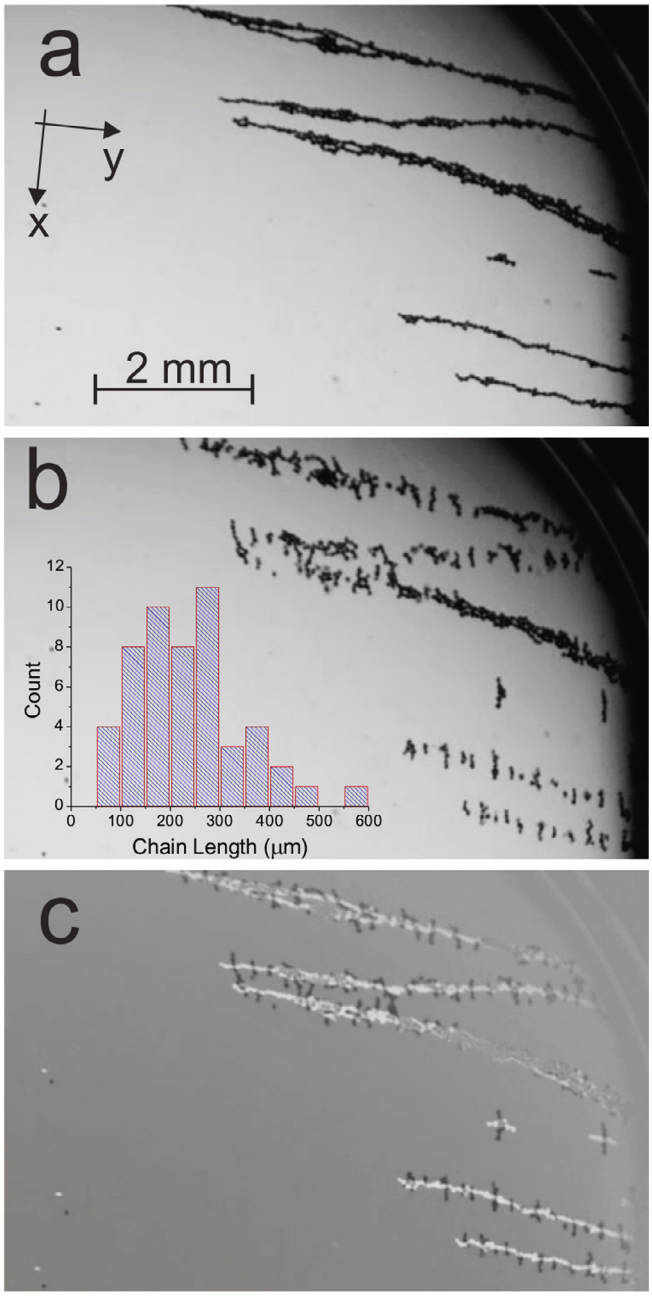

Fig. 3. a) Snapshot of self assembled chains for $B_{0z} = 1$ mT and $B_{0i} = 0.4$ mT. b) Snapshot immediately after rotating the plane containing the elliptically polarized field in $\frac{\pi}{2}$. The inset shows the chain lengths histogram for this snapshot. c) Superposition of both a) and b) snapshots showing the rotation of chain segments around their center of mass. For clarity, the initial chains are shown in light grey and the segments in dark grey lines. See text

In the main panel of Fig. 4 we plot the number of particle chains N registered in consecutive numbered frames, as a function of time, for cases where the total number of particles (the total area of dark pixels) is conserved. The typical length of the chain segments increases as N decreases over time. This result indicates that the particles agglomerate forming longer chains, actively stimulated by the rotating field [34].

Successive chain fragmentation and recombination was examined: Particles gradually reorganize in the steady applied AC magnetic field, and after a given time interval a new $\frac{\pi}{2}$ field rotation is applied. The peaks in N indicate high chain fragmentation, *i.e.* large number of short chains, and occur after each sudden plane field rotation. Alternating breakup and reformation of the particle chains is shown in Fig. 4 where short vertical arrows indicate the field rotation. Points labeled a) and b) correspond to the snapshots shown in Fig. 3 a) and b) respectively. It is interesting to note that reformation from fragments to longer chains occurs approximately in a power law time regime as was found in Ref. [34] for clustering of Ni and Fe micrometer-sized particles dispersed in a fluid under the action of rotating magnetic fields. Following these findings, the time decay of N (for the interval 9 s—13 s) was fitted to a power law function $N(t) \propto (t - t_0)^{-\alpha}$. that resulted satisfactory with $\alpha = 0.422$, as shown in the red line in the figure.

The controlled rotational dynamics of a single magnetic particle chain in an infinite fluid domain was addressed experimentally [35] and theoretically [36]. A diluted uniformly distributed super-

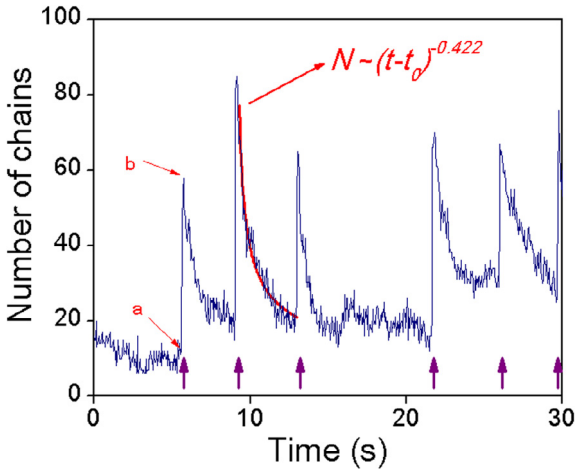

Fig. 4. Number of particle chains N registered in consecutive frames and plotted *vs* time. The rapid increase in N (chain fragmentation) correlates with every sudden change in the orientation of the plane containing the magnetic field vector, indicated in the figure by short vertical arrows. The time decay of N (for the interval 9 s—13 s) was fitted to a power law function (see text) shown in red line. Points a and b indicate the time position of the snapshots shown in Fig. 3 a) and b) respectively.

paramagnetic colloidal suspension was exposed to a strong, DC magnetic field until the suspended magnetic particles formed isolated magnetic particle chains, parallel to the field direction. The magnetic field was then rotated and the isolated chains rotated in order to remain oriented in the field with the field. Observations and calculations showed that for low viscous drag the complete chain rotates as a rigid rod following the field. But, as the viscous drag torque increases above the driven magnetic torque, the chain periodically fragments and reforms [32,37]. Although our present experimental array is different, a qualitative similar process may be leading to fragmentation.

4. Conclusions

We have studied the propulsion of soft magnetic particles dispersed in a viscous fluid upon the application of an elliptically polarized rotating magnetic field. Our approach was effective: we induced particle sedimentation by slightly reducing the surface tension of water and allowed the particles to interact with the confining plate through hydrodynamic flow provoked by magnetically assisted particle rotation. We found that above a low cross over vertical magnetic field, $\sim$1 mT magnetically assembled doublets move faster than single particles. We showed that the abrupt rotation of the magnetic field from the $x-z$ to $y-z$ plane and *vice versa* drives particles to describe complex controlled trajectories. The effect of the field rotation on long self assembled chains produces and alternating very fast breakup and power time law reformation of particle chains, similar to the behavior of other clustering mechanisms in magnetic colloidal suspensions. The chains break up in short segments that rotate around their center of mass to align in the new field direction, keeping the centre of mass in its original chain position. In future work a gradual plane rotation would allow control of the trajectories geometry, making this strategy promissory for applications in cargo delivery by single particles or by doublets, or in microfluids stirring.

Acknowledgement

The authors are grateful to I. S. Aranson for helpful discussions and for providing the magnetic microparticles. GAJ and MAL acknowledge support of the *Universidad Nacional de General Sarmiento*, CONICET (PIO CONICET UNGS-144-20140100016-CO), and ANPCyT (PICT2013-160). VB was supported by *Universidad de Buenos Aires* under grant UBAcyt 661 and CONICET under grant PIP 536.

References

[1] J.E. Avron, O. Gat, O. Kenneth, Optimal swimming at low reynolds numbers, Phys. Rev. Lett. 93 (2004) 186001.
[2] R. Golestanian, A. Ajdari, Mechanical response of a small swimmer driven by conformational transitions, Phys. Rev. Lett. 100 (2008) 038101.
[3] A. Najafi, R. Golestanian, Simple swimmer at low reynolds number: three linked spheres, Phys. Rev. E 69 (2004) 062901.
[4] C.M. Pooley, A.C. Balazs, Producing swimmers by coupling reaction-diffusion equations to a chemically responsive material, Phys. Rev. E 76 (2007) 016308.
[5] R. Dreyfus, J. Baudry, M.L. Roper, M. Fermigier, H.A. Stone, J. Bibette, Microscopic artificial swimmers, Nature 437 (7060) (2005) 862–865.
[6] F.Y. Ogrin, P.G. Petrov, C.P. Winlove, Ferromagnetic microswimmers, Phys. Rev. Lett. 100 (2008) 218102.
[7] D.C. Rapaport, Microscale swimming: the molecular dynamics approach, Phys. Rev. Lett. 99 (2007) 238101.
[8] J.E. Avron, O. Raz, A geometric theory of swimming: purcell's swimmer and its symmetrized cousin, N. J. Phys. 10 (6) (2008) 063016.
[9] A. Leshansky, O. Kenneth, Surface tank treading: propulsion of purcells toroidal swimmer, Phys. Fluids 20 (6) (2008) 063104.
[10] O. Raz, A. Leshansky, Efficiency of cargo towing by a microswimmer, Phys. Rev. E 77 (5) (2008) 055305.
[11] A. Kaiser, A. Snezhko, I.S. Aranson, Flocking ferromagnetic colloids, Sci. Adv. 3 (2) (2017) e1601469.
[12] M. Driscoll, B. Delmotte, M. Youssef, S. Sacanna, A. Donev, P. Chaikin, Unstable fronts and motile structures formed by microrollers, Nat. Phys. 13 (2017) 375–379.
[13] T. Prozorov, D.A. Bazylinski, S.K. Mallapragada, R. Prozorov, Novel magnetic nanomaterials inspired by magnetotactic bacteria: topical review, Mater. Sci. Eng.: R 74 (5) (2013) 133–172.
[14] S. Sudo, S. Segawa, T. Honda, Magnetic swimming mechanism in a viscous liquid, J. Intelligent Mater. Syst. Struct. 17 (8–9) (2006) 729–736.
[15] S. Guo, Q. Pan, M.B. Khamesee, Development of a novel type of microrobot for biomedical application, Microsyst. Technol. 14 (3) (2008) 307–314.
[16] B.J. Nelson, I.K. Kaliakatsos, J.J. Abbott, Microrobots for minimally invasive medicine, Ann. Rev. Biomed. Eng. 12 (2010) 55–85.
[17] S.T. Chang, V.N. Paunov, D.N. Petsev, O.D. Velev, Remotely powered self-propelling particles and micropumps based on miniature diodes, Nat. Mater. 6 (3) (2007) 235–240.
[18] J. Edd, S. Payen, B. Rubinsky, M. Stoller, M. Sitti, Proceedings of ieee/rsj international conference on intelligent robots and systems, 2003.
[19] S. Kim, F. Qiu, S. Kim, A. Ghanbari, C. Moon, L. Zhang, B.J. Nelson, H. Choi, Fabrication and characterization of magnetic microrobots for three-dimensional cell culture and targeted transportation, Adv. Mater. 25 (41) (2013) 5863–5868.
[20] A. Snezhko, I. Aranson, W.-K. Kwok, Dynamic self-assembly of magnetic particles on the fluid interface: surface-wave-mediated effective magnetic exchange, Phys. Rev. E 73 (4) (2006) 041306.
[21] A. Snezhko, I. Aranson, W.-K. Kwok, Surface wave assisted self-assembly of multidomain magnetic structures, Phys. Rev. Lett. 96 (7) (2006) 078701.
[22] J. Happel, H. Brenner, Low Reynolds number hydrodynamics: with special applications to particulate media, vol. 1, 2012.
[23] E.M. Purcell, Life at low reynolds number, Am. J. Phys. 45 (1) (1977) 3–11.
[24] A.J. Goldman, R.G. Cox, H. Brenner, Slow viscous motion of a sphere parallel to a plane wall–i motion through a quiescent fluid, Chem. Eng. Sci. 22 (4) (1967) 637–651.
[25] J. Schindelin, C.T. Rueden, M.C. Hiner, K.W. Eliceiri, The imagej ecosystem: an open platform for biomedical image analysis, Mol. Reprod. Develop. 82 (7–8) (2015) 518–529.
[26] Cuda video spot tracker. < http://cismm.web.unc.edu/>.
[27] Tracker video analysis tool. < http://physlets.org/tracker/>.
[28] M.N. Romodina, E.V. Lyubin, A.A. Fedyanin, Detection of brownian torque in a magnetically-driven rotating microsystem, Sci. Rep. 6.
[29] Q. Liu, A. Prosperetti, Wall effects on a rotating sphere, J. Fluid Mech. 657 (2010) 1–21.
[30] P. Tierno, O. Güell, F. Sagués, R. Golestanian, I. Pagonabarraga, Controlled propulsion in viscous fluids of magnetically actuated colloidal doublets, Phys. Rev. E 81 (1) (2010) 011402.
[31] P. Tierno, R. Golestanian, I. Pagonabarraga, F. Sagués, Controlled swimming in confined fluids of magnetically actuated colloidal rotors, Phys. Rev. Lett. 101 (21) (2008) 218304.
[32] I. Petousis, E. Homburg, R. Derks, A. Dietzel, Transient behaviour of magnetic micro-bead chains rotating in a fluid by external fields, Lab. Chip 7 (12) (2007) 1746–1751.
[33] F. Martinez-Pedrero, A. Ortiz-Ambriz, I. Pagonabarraga, P. Tierno, Colloidal microworms propelling via a cooperative hydrodynamic conveyor belt, Phys. Rev. Lett. 115 (13) (2015) 138301.
[34] M. Llera, J. Codnia, G.A. Jorge, Aggregation dynamics and magnetic properties of magnetic micrometer-sized particles dispersed in a fluid under the action of rotating magnetic fields, J. Magn. Magn. Mater. 384 (2015) 93–100.
[35] S. Melle, G.G. Fuller, M.A. Rubio, Structure and dynamics of magnetorheological fluids in rotating magnetic fields, Phys. Rev. E 61 (4) (2000) 4111.
[36] Y. Gao, M. Hulsen, T. Kang, J. den Toonder, Numerical and experimental study of a rotating magnetic particle chain in a viscous fluid, Phys. Rev. E 86 (4) (2012) 041503.
[37] S.L. Biswal, A.P. Gast, Rotational dynamics of semiflexible paramagnetic particle chains, Phys. Rev. E 69 (4) (2004) 041406.